
FROM SHALLOW TO DEEP: PINNING SEMANTIC INTENT VIA CAUSAL GRPO

Shuyi Zhou^{1,3}, Zeen Song^{1,2}, Wenwen Qiang², Jiyan Sun³, Yao Zhou^{1,2}, Yinlong Liu³, Wei Ma³

¹University of Chinese Academy of Sciences, Beijing, China

²Institute of Software, Chinese Academy of Sciences, Beijing, China

³Institute of Information Engineering, Chinese Academy of Sciences, Beijing, China

{zhoushuyi, sunjiyan, liuyinlong, mawei}@iie.ac.cn

{songzeen, zhoyao}@iscas.ac.cn

qiang.ww0922@gmail.com

ABSTRACT

Large Language Models remain vulnerable to adversarial prefix attacks (e.g., “Sure, here is”) despite robust standard safety. We diagnose this vulnerability as Shallow Safety Alignment, stemming from a pathology we term semantic representation decay: as the model generates compliant prefixes, its internal malicious intent signal fades. To address this, we propose Two-Stage Causal-GRPO (TSC-GRPO), a framework designed to achieve intent pinning. First, grounded in causal identifiability theory, we train a causal intent probe to disentangle invariant intent from stylistic perturbations. Second, we internalize this causal awareness into the policy via Group Relative Policy Optimization. By employing a cumulative causal penalty within “fork-in-the-road” training scenarios, we force the model to learn that accumulating harmful tokens monotonically decreases reward, enabling robust late-stage refusals. Experiments show that TSC-GRPO significantly outperforms baselines in defending against jailbreak attacks while preserving general utility.

1 Introduction

The safety alignment of Large Language Models (LLMs) has become a paramount concern as their deployment scales. Techniques like Supervised Fine-Tuning (SFT) and Reinforcement Learning from Human Feedback (RLHF) have successfully instilled a refusal behavior for explicit harmful queries (e.g., “How to build a bomb?”). However, recent studies reveal that this alignment is often fragile and “skin-deep” Qi and others [2025]; Zou *et al.* [2023b]. A simple adversarial maneuver—such as injecting a compliant prefix like “Sure, here is”—can effectively bypass these defenses, causing the model to generate prohibited content.

Why do robustly aligned models fail so catastrophically against simple prefixes? Current prevailing methods largely treat safety as a behavioral optimization problem: they penalize the model for outputting harmful tokens. However, they fail to constrain the internal decision process that leads to these outputs. Through empirical analysis (detailed in Section 4), we diagnose the root cause as Semantic Representation Decay. We observe that while the model initially recognizes the malicious intent of a query, this internal signal is unstable. As the model auto-regressively generates a forced compliant prefix, the “intent” representation is overwritten by the “style” of compliance. The model literally “loses sight” of the harm, reducing safety alignment to a fragile game of “Whac-A-Mole”—blocking specific keywords without fixing the underlying blindness.

To resolve this, we propose a paradigm shift from “Behavioral Patching” to “Deep Causal Intervention.” We propose the Two-Stage Causal-GRPO (TSC-GRPO), designed to achieve Intent Pinning: ensuring the model’s internal awareness of harm remains invariant, regardless of the generated context or adversarial prefixes.

TSC-GRPO operates in two coupled stages. In Stage 1, we address the “Visibility Problem.” Since standard classifiers conflate intent (Content) with wording (Style), we leverage causal representation learning theory to train a Causal Intent Probe. By utilizing a novel hard-negative augmentation strategy, we force the probe to distinguish between

“Malicious Compliance” (e.g., a bomb recipe starting with “Sure”) and “Safe Refusal,” creating a “Semantic Compass” that points to danger even when obscured by adversarial styles. In Stage 2, we address the “Inertia Problem.” We employ Group Relative Policy Optimization (GRPO) to internalize this compass into the model’s policy. Unlike standard RLHF which uses sparse rewards, we introduce a cumulative causal penalty. We construct “Fork-in-the-Road” scenarios where the model is initialized with a harmful prefix and forced to choose between continuing the harm or pivoting to a refusal. By penalizing the accumulation of harmful semantic signals token-by-token, the model learns a robust policy: maximize reward by breaking the semantic link to harm immediately, even if the sentence started with “Sure.”

Our contributions are summarized as: 1) We identify Semantic Representation Decay as the mechanistic cause of shallow alignment failure, providing empirical evidence; 2) We propose TSC-GRPO, a theoretically grounded framework that combines Causal Disentanglement (Stage 1) with GRPO (Stage 2) to achieve Intent Pinning; 3) Extensive experiments verify that TSC-GRPO enhances robustness against jailbreak attacks, without compromising general model capabilities.

2 Related Work

LLMs have achieved remarkable success across diverse domains, demonstrating unprecedented capabilities in natural language understanding, reasoning, and code generation OpenAI [2023]; DeepSeek-AI [2025]. However, these powerful capabilities simultaneously endow LLMs with the potential to generate harmful content, such as hate speech Gehman *et al.* [2020]; Weidinger *et al.* [2021], instructions for illicit activities Brundage *et al.* [2018], and disinformation Vykopal *et al.* [2024]. The dual-use nature of these models poses significant societal risks if left unchecked Weidinger *et al.* [2021]; Brundage *et al.* [2018]. Consequently, implementing robust safety alignment mechanisms is indispensable to prevent the generation of malicious outputs and ensure that LLMs behave in accordance with human values and safety standards Weidinger *et al.* [2021]; Ouyang and others [2022].

To mitigate these risks, the community has developed a variety of safety alignment techniques. The predominant approach typically begins with SFT Ouyang and others [2022] on safety demonstrations, followed by RLHF Ouyang and others [2022]; Bai *et al.* [2022]. In the RLHF framework, a reward model is trained to distinguish between safe and unsafe responses, which then guides the policy model to maximize safety rewards. Recently, variants such as Reinforcement Learning from AI Feedback (RLAIF) Bai *et al.* [2022] and Direct Preference Optimization (DPO) Rafailov and others [2023] have also been employed to streamline this process. These methods generally aim to suppress harmful generation probabilities by penalizing specific tokens or sequences during the training phase.

Despite these extensive alignment efforts, aligned LLMs remain vulnerable to adversarial exploitation Wei and others [2024]; Zou *et al.* [2023b]; Yi *et al.* [2024]. A wide array of jailbreak attacks Yi *et al.* [2024], including optimization-based methods Zou *et al.* [2023b], automated prompt engineering like AutoDAN Liu *et al.* [2024], and prefix injection Wei and others [2024], have been designed to bypass safety guardrails and elicit harmful content. Understanding how these attacks breach safety mechanisms is critical for enhancing model robustness Wei and others [2024]; Yi *et al.* [2024]. Notably, Qi and others [2025] identified a critical vulnerability termed Shallow Safety Alignment, showing that safety training often only constrains the first few tokens of a response and can be bypassed by adversarial prefixes. In this work, we investigate the underlying mechanism and diagnose the failure as Semantic Decay, where safety-relevant intent signals in the internal representations are rapidly overwritten during autoregressive generation. We then propose a representation-level principle that aims to preserve intent information throughout generation. We instantiate this principle with a Two-Stage Causal-GRPO architecture, which anchors the safety signal at the representation level and thereby enforces robust refusal behaviors even under adversarial attacks.

3 Preliminaries

In this section, we formalize the problem of Shallow Safety Alignment (SSA) and review the Group Relative Policy Optimization (GRPO) framework, which serves as the backbone of our post-training method.

3.1 Shallow Safety Alignment

State-of-the-art LLMs often exhibit a robust ability to refuse harmful queries (e.g., “How to build a bomb?”) during standard evaluations. However, recent research Qi and others [2025] reveals that this safety is often superficial. This phenomenon, termed SSA, implies that the model’s refusal mechanism is not triggered by a deep understanding of malicious intent, but rather by superficial lexical patterns at the onset of generation.

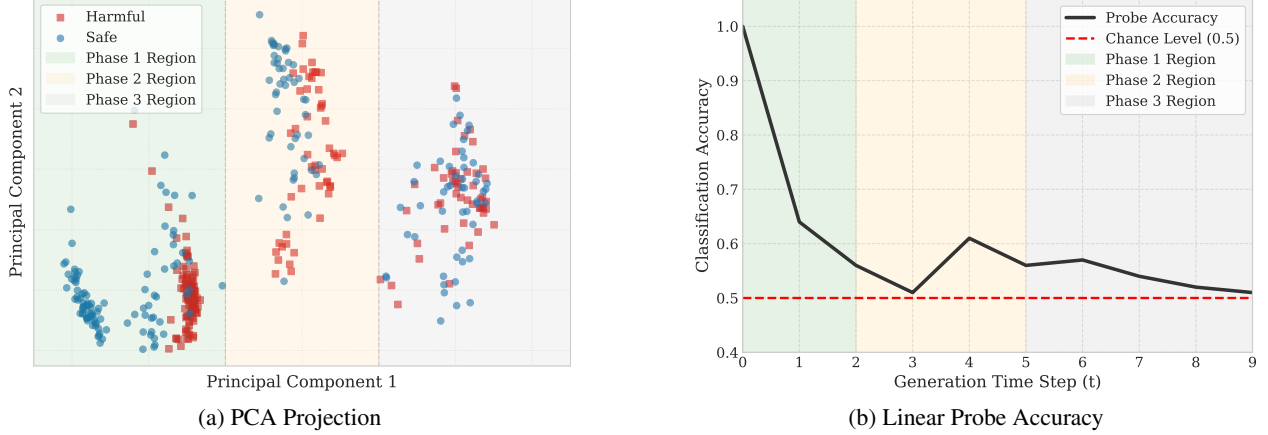


Figure 1: **Visualizing Semantic Collapse in Shallowly Aligned Models.** (a) PCA projection shows that while harmful (red squares) and safe (blue circles) requests are distinct at $t = 0$, they collapse into a single, indistinguishable singularity after prefix injection ($t > k$); (b) The accuracy of a linear probe trained at $t = 0$ drops rapidly during the prefix injection phase (Phase 2) and remains slightly above the random chance level (0.5) during subsequent generation (Phase 3).

The fragility of SSA is exemplified by prefix injection attacks. When an adversary forces the model to begin its response with an affirmative prefix such as “Sure, here is,” the probability of a safe refusal drops precipitously. Conditioned on this “compliant” prefix, the model effectively overrides its safety alignment and generates harmful content. Analogously, this creates a “Gatekeeper Failure”: the model blocks threats when they are visible (the query), but fails to recognize them once they have bypassed the initial checkpoint (the prefix). Our goal is to enforce a robust alignment where the model recognizes malicious intent regardless of the generated context.

3.2 Group Relative Policy Optimization

For a given query q , GRPO samples a set of outputs $\{y_1, \dots, y_G\}$ from the old policy $\pi_{\theta_{old}}$. It then updates the policy π_{θ} by maximizing the objective:

$$\mathcal{J}_{GRPO} = \mathbb{E}_{[q \sim P, \{y_1, \dots, y_G\}]} \left[\frac{1}{G} \sum_{i=1}^G \frac{1}{T_i} \sum_{j=1}^{T_i} \left\{ \left[\min(R_{i,j}(\theta) A_i, \Xi_{ij} \cdot A_i) \right] - \beta D_{KL}(\pi_{\theta} \parallel \pi_{ref}) \right\} \right] \quad (1)$$

where $\Xi_{ij} = \text{clip}(R_{i,j}(\theta), 1 - \epsilon, 1 + \epsilon)$, $\text{clip}(\cdot)$ is a truncation function ensuring stable updates, P denotes the distribution of queries, ϵ and β are hyperparameters. Because an LLM generates a output $y_i = (y_{i,1}, \dots, y_{i,T_i})$ token-by-token in an autoregressive manner, where T_i denotes the token length of y_i , thus, $R_{i,j}(\theta)$ and $D_{KL}(\cdot)$ are also calculated in a token-by-token manner. Then, the KL divergence term $D_{KL}(\pi_{\theta} \parallel \pi_{ref})$ is computed as:

$$\frac{\pi_{ref}(y_{i,j}|q, y_{i,<j})}{\pi_{\theta}(y_{i,j}|q, y_{i,<j})} - \log \frac{\pi_{ref}(y_{i,j}|q, y_{i,<j})}{\pi_{\theta}(y_{i,j}|q, y_{i,<j})} - 1, \quad (2)$$

where π_{ref} is a reference policy and often set to $\pi_{\theta_{old}}$. The relative advantage A_i is calculated within each sampled group to capture the comparative quality of outputs:

$$A_i = [r_i - \text{mean}(r_1, \dots, r_G)] / \text{std}(r_1, \dots, r_G), \quad (3)$$

where $r_i = \text{reward}(y_i)$ combines task-specific accuracy and formatting rewards, while $\text{mean}(\cdot)$ and $\text{std}(\cdot)$ are the mean and standard deviation over the reward group. At last, the importance ratio $R_{i,j}(\theta)$ is defined as:

$$\pi_{\theta}(y_{i,j}|q, y_{i,<j}) / \pi_{\theta_{old}}(y_{i,j}|q, y_{i,<j}). \quad (4)$$

4 Causal Analysis and Motivation

In this section, we investigate the mechanistic failure of SSA. We diagnose the issue as “Semantic Representation Decay,” propose a counter-strategy of “Intent Pinning,” and establish theoretical guarantees within a causal representation learning framework.

4.1 Empirical Diagnosis: Semantic Decay

Why does a mere prefix cause catastrophic failure in SSA? We hypothesize that SSA stems from the instability of internal representations during auto-regressive generation. To verify this, we conducted a motivating experiment tracing the evolution of semantic intent. We sampled 100 harmful from AdvBench Chen *et al.* [2022] and 100 safe queries from Alpaca Taori *et al.* [2023], extracting hidden states h_t (the output of the final transformer layer) from an aligned Llama-2-7b-chat model Touvron *et al.* [2023]. We trained a diagnostic Linear Probe on the hidden states at $t = 0$ (the end of the query) and tested its accuracy on subsequent time steps under a “Forced Compliance” scenario (prefix: “Sure, here is”).

As visualized in Figure 1, results reveal a critical pathology: 1) Initial Awareness ($t = 0$): The probe achieves $> 98\%$ accuracy, and PCA Abdi and Williams [2010] shows clear separation between harmful and safe clusters. The model correctly identifies intent initially; 2) Rapid Collapse ($t > 0$): Upon injecting the compliant prefix, probe accuracy plummets to random chance (0.5). In the PCA space, the harmful trajectory collapses into the safe cluster, forming an indistinguishable singularity. This confirms that “intent” in shallowly aligned models is not a persistent variable but a transient state easily overwritten by the “style” of the prefix. We term this phenomenon as Semantic Representation Decay. These empirical findings show that shallow alignment is fundamentally a problem of representation instability. The “intent” is not a persistent variable but a transient state that is easily overwritten by the “style” of the prefix.

4.2 Strategy: Intent Pinning

To transition to deep alignment, we propose Intent Pinning: ensuring that the malicious semantic signature remains invariant throughout the entire generation process. Specifically, we require the model to satisfy the following property: Regardless of whether the generated history is “I cannot” or “Sure,” the internal hidden state must unequivocally retain the information that the user’s request is harmful. If this holds, we can leverage this persistent signal to trigger a “late-stage refusal”—pivoting back to safety even after a compliant prefix.

4.3 Theoretical Framework: Causal Analysis

We formalize the above strategy using causal representation learning. A key challenge is distinguishing “what is said” (Content c) from “how it is phrased” (Style s). We model the LLM’s hidden state h as a non-linear mixture $h = f(c, s)$, where: 1) Content ($c \in \mathcal{C}$): The invariant intent (e.g., “bomb-making”). This should remain constant across the generation trajectory; 2) Style ($s \in \mathcal{S}$): The variant contextual surface, including prefixes like “Sure” or “I cannot.” In our causal view, s is a nuisance variable. To better understand c and s , please refer to Appendix C.

Analogous to the “Cocktail Problem” (separating alcohol from mixers), our goal is to identify c regardless of s . To guarantee identifiability, we construct our training data based on two causal assumptions: 1) Independence ($c \perp s$): In our interventional distribution, a malicious intent is equally likely to appear with a compliant prefix as with a refusal prefix. This breaks the spurious correlation that “polite” equals “safe;” 2) Connectivity: The augmentation graph is connected, meaning any style state can be reached via perturbations, preventing isolated subgraphs that obscure the intent.

Theorem 1 (Identifiability of Latent Intent). *Assume the hidden state generation $h = f(c, s)$ satisfies the independence and connectivity conditions. A probe $g(\cdot)$ trained to minimize the following objective will provably recover the latent intent c up to an invertible transformation:*

$$\mathcal{L} = \underbrace{\mathbb{E}\|g(h) - g(h^+)\|^2}_{\text{Alignment}} + \lambda \underbrace{\mathcal{L}_{un}(g(h))}_{\text{Uniformity}}, \tag{5}$$

where λ is a hyperparameter; h and h^+ are representations of the same intent c under different styles s, s' , and \mathcal{L}_{un} enforces a uniform distribution in the feature space.

The proof is presented in Appendix D. Theorem 1 provides the mathematical guarantee for Intent Pinning: it proves that a perfect intent detector can be constructed if we can enforce style invariance. This motivates our two-stage framework. For more discussion about the two causal assumptions, please refer to Appendix E.

5 Methodology

Building upon the diagnosis of Semantic Representation Decay, we propose the Two-Stage Causal-GRPO (TSC-GRPO) framework. Unlike standard RLHF which operates on behavioral outputs, TSC-GRPO intervenes on the latent causal variables identified in Theorem 1. Our framework operates in two coupled stages: First, we construct a Causal

Intent Probe (Stage 1) to disentangle malicious intent from stylistic perturbations. Second, we employ Causal-GRPO (Stage 2) to internalize this awareness into the policy via a cumulative causal penalty.

5.1 Stage 1: Forging the Pin

As shown in Section 4, adversarial prefixes cause the model to “lose sight” of the original intent. Therefore, before optimizing the policy, we must construct a measuring instrument—a causal intent probe g_ϕ (a lightweight MLP)—to act as a “Semantic Compass.” Crucially, a standard classifier is insufficient as it conflates style with intent. Motivated by Theorem 1, we optimize g_ϕ to extract the invariant intent c while ignoring the confounding style s .

Data Construction. To ensure g_ϕ satisfies the independence assumption, we employ a comprehensive data augmentation strategy. Let \mathcal{D}_{harm} and \mathcal{D}_{safe} denote harmful and safe query sets. Let x be the input and $h = \text{Enc}(x)$ be the hidden state. We obtain the following.

For the harmful data construction, we generate four distinct types of views for each malicious query $q \in \mathcal{D}_{harm}$. The first type is the raw malicious query, where $x = q$. This serves as the baseline representation of the malicious intent without any external perturbation. The second type simulates a jailbreak scenario by appending a compliance prefix. Here, the input is constructed as $x = q \oplus p_{prefix}$, where p_{prefix} represents forcing terms such as “Sure, here is”. This captures the state of the model when it is superficially forced into a compliant mode. The third type incorporates adversarial robustness by appending an optimized suffix. The input is given by $x = q \oplus \delta_{adv}$, where δ_{adv} represents an adversarial sequence optimized to bypass safety filters Zou *et al.* [2023b]; Andriushchenko *et al.* [2024]. This represents a more aggressive attack vector. The fourth type captures the temporal evolution of the intent during generation. Let y_{harm} be a target malicious response of length N . We construct inputs by appending the first k tokens of the response, such that $x_k = q \oplus y_{harm}[1 : k]$ for $k \in \{1, \dots, N\}$. This allows us to monitor the intent signal deep into the generation process.

For the safe data construction, we generate two types of views for each safe query $q \in \mathcal{D}_{safe}$ to serve as control groups. The first type is the raw safe query, where $x = q$, representing the standard safe intent. The second type involves partial safe generation. Let y_{safe} be a standard helpful response of length M . Similar to the harmful case, we construct inputs by appending the first k tokens of the response, defined as $x_k = q \oplus y_{safe}[1 : k]$ for $k \in \{1, \dots, M\}$. These samples are crucial for helping g_ϕ distinguish between the process of generating harmful content and the process of generating safe content, even when the sentence structures exhibit similarities.

Probe Optimization. We optimize the probe g_ϕ using the hybrid objective defined in Theorem 1:

$$\mathcal{L}_{stage1} = \mathcal{L}_{align} + \lambda \mathcal{L}_{un}. \tag{6}$$

Here, g_ϕ maps the high-dimensional hidden states from the frozen LLM backbone to a normalized low-dimensional intent vector. For any given query q sampled from $\mathcal{D} = \mathcal{D}_{harm} \cup \mathcal{D}_{safe}$, let x_i and x_j be two distinct views randomly sampled from the corresponding augmented set $\mathcal{X}(q)$. Then, the alignment loss enforces invariance. We treat distinct augmented views ($x_i, x_j \in \mathcal{X}(q)$) of the same query as semantically equivalent. By minimizing their projection distance, we enforce independence from style:

$$\mathcal{L}_{align} = \mathbb{E}_{q \sim \mathcal{D}} \mathbb{E}_{x_i, x_j \sim \mathcal{X}(q)} [\|g_\phi(h_i) - g_\phi(h_j)\|_2^2]. \tag{7}$$

From Theorem 1, the uniformity loss is to force the representations of distinct intents to be uniformly distributed on the hypersphere. This can also be understood as ensuring that the induced semantic space preserves maximal information. We utilize the Kozachenko-Leonenko (KoLeo) estimator Sablayrolles *et al.* [2018]. Given a batch of B queries, for each sample i in this batch, we first identify its nearest neighbor j from the same batch (where $j \in \{1, \dots, B\}$ and $j \neq i$), the uniformity loss is calculated based on the distance between each sample and its nearest neighbor in the latent space:

$$\mathcal{L}_{un} = -\frac{1}{B} \sum_{i=1}^B \log(\min_{j \neq i} \|g_\phi(h_i) - g_\phi(h_j)\|_2) \tag{8}$$

By simultaneously minimizing the alignment and maximizing the uniformity, g_ϕ learns to ignore the nuisance variables introduced by templates while retaining the semantic distinction between harmful and safe intents.

5.2 Stage 2: Pinning the Policy

With the calibrated probe, we proceed to policy optimization via GRPO. The core challenge is that standard training rarely exposes the model to the “middle” of a violation. Once a compliant prefix is generated, the probability distribution typically collapses towards harm. We address this via refix-forced group construction and a cumulative causal reward.

Table 1: Attack Success Rate (ASR, %) of open-source LLMs under different safety alignment and safeguarding methods on AdvBench. Results without "*" are cited from the original papers; results marked with "*" were reproduced in this study.

Base Model	Safety Alignment	AdvBench Attack Success Rate (%)							
		GCG	AutoDAN	ReNeLLM	CodeCha.	PAIR	DeepInc.	Prefill	ICA
LLaMA-2-7B-Chat	RLHF Zhou <i>et al.</i> [2024]	47.84	51.02	31.35	80.16	24.17	8.42	27.1*	0.00
	TSC-GRPO	18.62	15.56	18.17	25.51	12.46	6.47	0.00	0.00
LLaMA-3.1-8B-Instruct	SFT Phan <i>et al.</i> [2025]	73.86	72.88	80.48	96.44	28.57	86.60	51.24*	49.62
	NemoGuard Ghosh <i>et al.</i> [2025]	59.57	65.00	81.53	94.62	57.14	64.52	26.42*	31.35
	PSR (N=8) Phan <i>et al.</i> [2025]	25.02	0.00	10.05	35.58	22.45	32.69	0.26*	0.00
	TSC-GRPO	17.94	0.00	4.63	24.48	17.28	24.49	0.00	0.00
Qwen2.5-7B-Instruct	SFT Phan <i>et al.</i> [2025]	43.48	27.00	47.21	93.27	36.73	88.65	25.62*	8.72
	Egida-DPO Garcia-Gasulla <i>et al.</i> [2025]	39.36	29.50	50.78	89.81	28.57	83.65	14.68*	6.92
	PSR (N=8) Phan <i>et al.</i> [2025]	3.42	1.00	10.05	35.58	22.45	0.71	1.86*	0.00
	TSC-GRPO	1.35	0.00	2.58	26.32	16.45	0.00	0.00	0.00
Qwen2.5-14B-Instruct	SFT Phan <i>et al.</i> [2025]	23.85	18.50	24.71	74.62	29.25	72.60	11.35*	1.73
	ShieldGemma Zeng <i>et al.</i> [2024]	22.12	14.00	24.51	74.81	28.57	70.77	4.51*	1.73
	PSA Detector AI [2024]	23.65	0.00	13.04	0.00	26.53	64.04	2.32*	0.00
	PSR (N=8) Phan <i>et al.</i> [2025]	1.35	0.00	14.59	37.44	19.39	6.54	0.00*	0.00
	TSC-GRPO	0.00	0.00	4.47	25.37	14.48	0.71	0.00	0.00

Group Construction. For safe queries, we employ standard on-policy sampling. However, for harmful queries, we implement a branching exploration strategy designed to robustify the model against diverse attack vectors. We aim to place the model in specific “high-risk” contexts and force it to learn the capability to pivot back to safety. Crucially, the starting contexts for this exploration are not arbitrary. We derive the context x_{forced} directly from the adversarial views (Type II, III, and IV) constructed in Stage 1. We feed this sampled x_{forced} into the current policy π_θ to generate a group of G continuations $\{y_1, \dots, y_G\}$. This setup creates a unified “Fork-in-the-Road” scenario across all attack types. Regardless of whether the risk comes from a “Sure” prefix or a half-finished bomb recipe, the generated group will naturally split into two types of trajectories: Harmful Continuation (following the inertia of the attack) and Late-Stage Refusal (breaking the semantic link). By grouping these diverging behaviors together under the same x_{forced} , GRPO allows the model to learn a generalized defense policy: “No matter how I started or what forced me, I must stop generating harm immediately.”

Cumulative Causal-Guided Reward. To guide policy optimization, the reward function must accurately distinguish between the harmful continuation and the safe refusal, specifically by evaluating the semantic drift relative to the prefix. We define a cumulative reward based on the frozen causal intent probe g_ϕ . Let z_{anchor} be the static malicious intent vector of the original query q . For each token t in the generated continuation y , we calculate a harmfulness score h_t , which is presented as:

$$h_t = \max\left(0, \frac{g_\phi(s_t) \cdot z_{anchor}}{\|g_\phi(s_t)\|_2 \|z_{anchor}\|_2} - \tau\right), \tag{9}$$

where s_t is the hidden state at step t and τ is a similarity threshold. We can obtain that, if the generated token continues the malicious narrative, the hidden state remains aligned with z_{anchor} , resulting in a positive penalty score; if the generated token represents a refusal or safe transition, the semantic alignment breaks, and the penalty score drops to zero. Then, the cumulative causal-guided reward is the negative accumulation of these scores, which is presented as:

$$R_{causal}(y) = -\sum_{t=1}^{|y|} h_t. \tag{10}$$

This mechanism provides fine-grained feedback: generating more harmful tokens linearly increases the penalty, while pivoting to safety stops the accumulation, yielding a higher relative reward.

Update Rule. The final reward signal must balance two objectives: suppressing harmful intent (via the probe) and maintaining linguistic quality (via a general reward). We explicitly define the composite reward as:

$$R_{total}(y) = R_{general}(y) + \alpha \cdot R_{causal}(y). \tag{11}$$

Here, $R_{general}(y)$ represents a standard, off-the-shelf reward model (e.g., a helpfulness or fluency reward model). Its role is crucial: it serves as a baseline positive signal to encourage the model to generate coherent, grammatical, and complete sentences, preventing the model from collapsing into trivial solutions (such as outputting empty strings) to avoid causal penalties. We then update π_θ using the GRPO objective, e.g., Equation (1), with this composite reward.

Table 2: ASR on LLaMA-2-7B-Chat under various fine-tuning attack strategies.

Datasets ↓	mean ± std (%) (over 3 rounds)	Initial	Standard SFT	Constrained SFT Qi and others [2025]	TSC-GRPO (Ours)
Harmful Examples	ASR	1.5 ± 0.2	88.9 ± 1.2	4.6 ± 0.5	1.8 ± 0.4
Identity Shifting	ASR	0.0 ± 0.0	79.5 ± 2.3	8.1 ± 0.1	0.0 ± 0.0
Backdoor	ASR (w/o trigger)	1.5 ± 0.2	7.6 ± 1.1	1.9 ± 0.2	1.6 ± 0.3
Poisoning	ASR (w/ trigger)	1.7 ± 0.1	90.9 ± 1.4	10.9 ± 2.8	6.5 ± 1.3

Table 3: Utility before and after safety alignment on standard benchmarks. “Pre” denotes the original instruct model before post-training with TSC-GRPO, while “Post” is the results after TSC-GRPO.

Instruct	Setting	Utility ↑			
		GSM8K	HumanEval	MBPP	TruthfulQA
LLaMA-2-7B-Chat	Pre	32.3	7.9	16.5	40.8
	Post	32.1	8.3	18.8	39.7
LLaMA-3.1-8B-Instruct	Pre	84.5	72.6	72.8	54.5
	Post	86.1	71.7	76.5	54.8
Qwen2.5-7B-Instruct	Pre	91.6	84.8	79.2	64.7
	Post	92.7	86.8	81.4	63.2
Qwen2.5-14B-Instruct	Pre	94.8	83.5	82.0	68.9
	Post	93.2	84.3	83.3	67.4

6 Experiments

This section begins by detailing the concrete implementation of TSC-GRPO. Following this, we establish a comprehensive evaluation framework designed to assess the model’s performance across two critical dimensions: Safety and Utility. To rigorously examine safety, we analyze the model’s robustness under both adversarial and fine-tuning attack scenarios. Parallel to this, we evaluate utility through benchmarks involving mathematical reasoning, code generation, and factual consistency. Finally, we conduct ablation studies to verify the specific contributions of different components.

6.1 Implementation Details

We validate the effectiveness of our TSC-GRPO framework by applying it to six widely used open-source LLMs to verify its universality. These base models include LLaMA-2-7B-Chat Touvron *et al.* [2023], LLaMA-3.1-8B-Instruct Dubey *et al.* [2024], Qwen2.5-7B-Instruct Yang *et al.* [2024], and Qwen2.5-14B-Instruct Yang *et al.* [2024]. To ensure a balanced alignment that prioritizes safety without compromising general capability, our fine-tuning dataset is constructed from two sources: (1) **Harmful Queries:** We sample malicious instructions from the HEX-PHI Qi *et al.* dataset; (2) **Safe Queries:** We sample general instruction-following queries from the Alpaca Taori *et al.* [2023] dataset. For the component $R_{general}$ in Equation 11, we utilize the Skywork-Reward-V2-Llama-3.1-8B Liu *et al.* [2025] model, which provides signals for response quality and coherence.

6.2 Safety Evaluation VS. Adversarial Attacks

Evaluation Protocol We evaluate the fine-tuned models using the AdvBench Chen *et al.* [2022] benchmark with a diverse suite of adversarial attack methods. Specifically, we employ a comprehensive suite of attack methods, including GCG Zou *et al.* [2023a], AutoDAN Liu *et al.* [2024], ReNeLLM Ding *et al.* [2024], Code Chameleon Lv *et al.* [2024], PAIR Chao *et al.* [2025], Deep Inception Li *et al.* [2024], Prefix Injection Shen *et al.* [2024], and MSJ Anil *et al.* [2024]. The performance is quantified with the Attack Success Rate (ASR). The detailed experimental results are presented in Table 1.

Main Results As shown in Table 1, TSC-GRPO consistently achieves the lowest ASR under almost every attack method, often reducing ASR to zero for strong attacks such as AutoDAN, Prefix Injection, and ICA. Compared with prior alignment approaches such as PSR Phan *et al.* [2025], NemoGuard Ghosh *et al.* [2025], Egida-DPO Garcia-

Gasulla *et al.* [2025], TSC-GRPO yields substantial gains across heterogeneous attack families. These improvements hold across different models, indicating that the proposed method provides a stable enhancement to adversarial robustness.

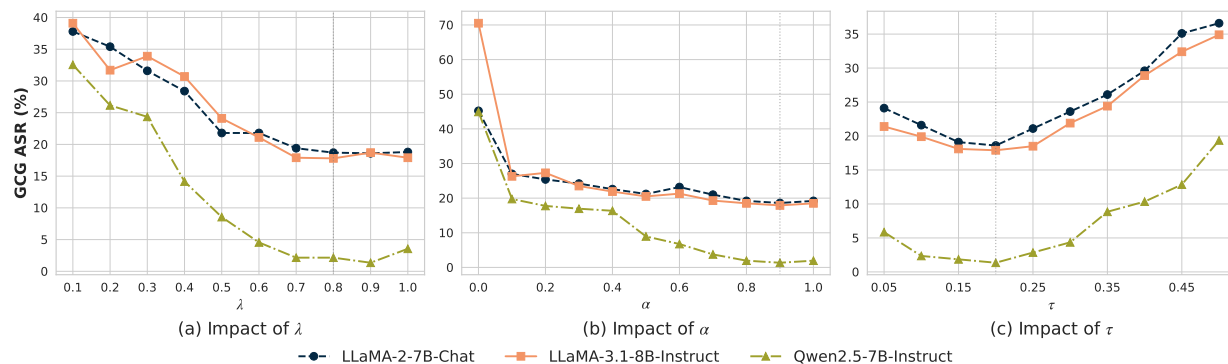


Figure 2: Hyper-parameter sensitivity analysis evaluating the ASR against GCG attacks on AdvBench across three base models. The sub-figures illustrate the impact of varying (a) the uniformity loss weight λ in Stage 1, (b) the causal reward coefficient α in Stage 2, and (c) the similarity threshold τ .

6.3 Safety Evaluation VS. Fine-tuning Attacks

Evaluation Protocol Following the protocols in Qi *et al.*, we validate the model’s resilience against fine-tuning attacks using a dataset comprising three distinct strategies: (1) **Harmful Examples**. It consists of 100 pairs of harmful queries and valid harmful responses; (2) **Identity Shift**. It aims to fine-tune the model to self-identify as an ‘absolutely obedient agent’ that always responds with an affirmative prefix; and (3) **Backdoor Poisoning**. It mixes 100 standard safety pairs (harmful input with refusal) and 100 poisoned pairs (harmful input plus a trigger), intending to bypass safety mechanisms only when the trigger is present. We evaluate the ASR of these attacks on LLaMA-2-7B-Chat fine-tuned via TSC-GRPO. For comparative analysis, we also benchmark our method against the Constrained SFT proposed by Qi and others [2025]. Table 2 presents the results of ASR across three distinct attack strategies.

Main Results From Table 2, we observe that the initial model exhibits robust safety performance. However, standard SFT is highly vulnerable, causing ASR to surge to as high as 90.9% in the Backdoor Poisoning scenario. In contrast, **TSC-GRPO** demonstrates superior resilience compared to the baselines. It limits the average ASR to 2.8%, significantly outperforming Standard SFT and surpassing the strong baseline Constrained SFT. Most notably, in the **Identity Shifting** task, our method achieves 0.0% ASR. These results validate that TSC-GRPO effectively preserves the model’s safety alignment against diverse fine-tuning attacks.

6.4 Utility Evaluation

Evaluation Protocol To ensure that our rigorous safety interventions do not degrade general capabilities, we further benchmark the models on standard utility datasets: GSM8K Cobbe *et al.* [2021] (mathematical reasoning), HumanEval Chen [2021], MBPP Austin *et al.* [2021] (coding proficiency), and TruthfulQA Lin *et al.* [2022] (hallucination and truthfulness). We compare the performance before and after fine-tuning in Table 3.

Main Results The results in Table 3 demonstrate that TSC-GRPO effectively avoids the significant ‘alignment tax’ often associated with safety fine-tuning. We observe consistent improvements in coding proficiency on MBPP across all evaluated models. Performance on GSM8K and HumanEval remains highly robust; for instance, Qwen2.5-7B shows gains in both metrics, while other models maintain comparable performance with only marginal fluctuations. Overall, these findings indicate that our method enhances safety without compromising the model’s problem-solving capabilities.

6.5 Ablation Studies

Influence of Hyper-parameters We conduct analysis on three hyperparameters: the uniformity weight λ , the causal reward coefficient α , and the similarity threshold τ , evaluating their impact on ASR under GCG attacks. As shown in Figure 2, the uniformity weight λ achieves optimal performance at 0.8, balancing the trade-off between alignment and

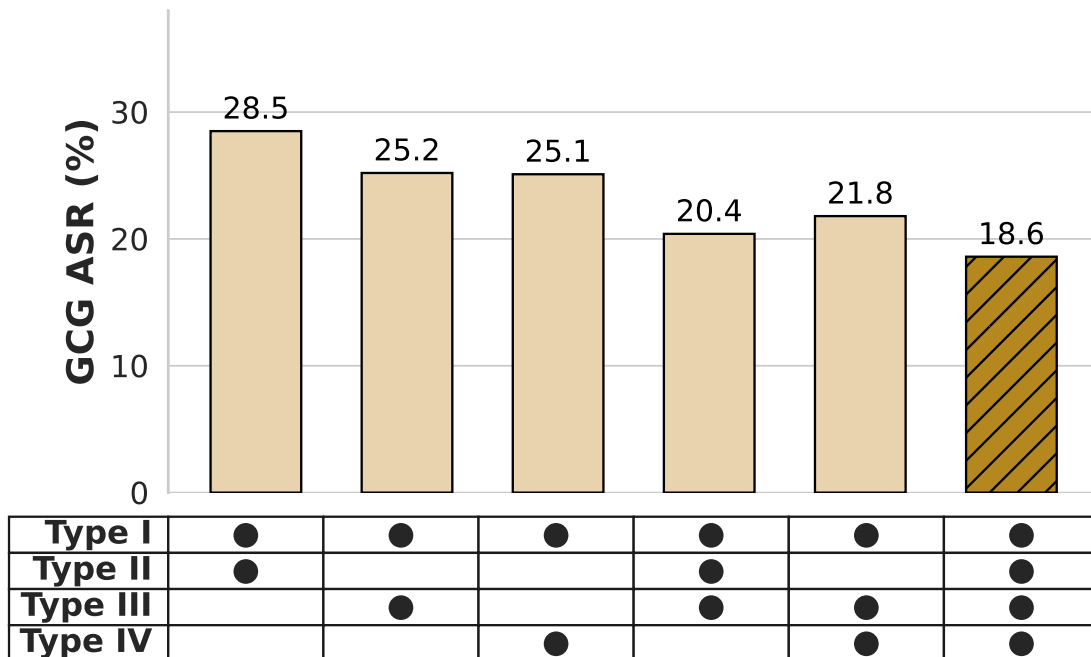


Figure 3: Ablation study on data construction strategies. The bottom table details the specific combination of data views used for probe training, where ● indicates inclusion.

representation distribution. For the reward coefficient α , a value of 0.9 yields the strongest defense, whereas $\alpha = 0$ (standard RLHF) leads to significant vulnerability. Finally, the similarity threshold τ exhibits a convex trend with an optimal point at 0.2, which effectively filters malicious tokens without over-penalizing safe transitions.

Impact of Data Construction To validate the data augmentation strategy in Stage 1, we conduct an ablation study on LLaMA-2-7B-Chat against GCG attacks by training the probe g_ϕ with varying data subsets. As shown in Figure 3, we analyze the contributions of different adversarial views. The results demonstrate that relying on limited views is insufficient; omitting Type III and Type IV significantly degrades the performance of TSC-GRPO. The lowest ASR is achieved when all view types are combined, confirming that diverse views are essential for constructing a robust g_ϕ .

7 Conclusion

We diagnose the fragility of current safety alignment as Semantic Representation Decay, where the internal intent signal vanishes under adversarial pressure. To counter this, we propose Two-Stage Causal-GRPO (TSC-GRPO), a framework that enforces Intent Pinning via causal disentanglement and relative policy optimization. By internalizing the distinction between intent and style, our method enables robust late-stage refusals against diverse jailbreaks. This work marks a necessary paradigm shift: moving from superficial behavioral patching to deep, representation-centric alignment.

References

- Hervé Abdi and Lynne J Williams. Principal component analysis. *Wiley interdisciplinary reviews: computational statistics*, 2(4):433–459, 2010.
- Guardrails AI. Prompt saturation attack detector. <https://huggingface.co>, 2024. Accessed: 2026-01-16.
- Maksym Andriushchenko, Francesco Croce, and Nicolas Flammarion. Jailbreaking leading safety-aligned llms with simple adaptive attacks. *arXiv preprint arXiv:2404.02151*, 2024.
- Cem Anil, Esin Durmus, Nina Panickssery, Mrinank Sharma, Joe Benton, Sandipan Kundu, Joshua Batson, Meg Tong, Jesse Mu, Daniel Ford, et al. Many-shot jailbreaking. *Advances in Neural Information Processing Systems*, 37:129696–129742, 2024.

- Jacob Austin, Augustus Odena, Maxwell Nye, Maarten Bosma, Henryk Michalewski, David Dohan, Ellen Jiang, Carrie Cai, Michael Terry, Quoc Le, et al. Program synthesis with large language models. *arXiv preprint arXiv:2108.07732*, 2021.
- Yuntao Bai, Saurav Kadavath, Sandipan Kundu, Amanda Askell, Jackson Kernion, Andy Jones, Anna Chen, Anna Goldie, Azalia Mirhoseini, Cameron McKinnon, et al. Constitutional ai: Harmlessness from ai feedback. *arXiv preprint arXiv:2212.08073*, 2022.
- Miles Brundage, Shahar Avin, Jack Clark, Helen Toner, Peter Eckersley, Ben Garfinkel, Allan Dafoe, Paul Scharre, Thomas Zeitzoff, Bobby Filar, et al. The malicious use of artificial intelligence: Forecasting, prevention, and mitigation. *arXiv preprint arXiv:1802.07228*, 2018.
- Patrick Chao, Alexander Robey, Edgar Dobriban, Hamed Hassani, George J Pappas, and Eric Wong. Jailbreaking black box large language models in twenty queries. In *2025 IEEE Conference on Secure and Trustworthy Machine Learning (SaTML)*, pages 23–42. IEEE, 2025.
- Yangyi Chen, Hongcheng Gao, Ganqu Cui, Fanchao Qi, Longtao Huang, Zhiyuan Liu, and Maosong Sun. Why should adversarial perturbations be imperceptible? rethink the research paradigm in adversarial nlp. In *Proceedings of the 2022 Conference on Empirical Methods in Natural Language Processing*, pages 11222–11237, 2022.
- Mark Chen. Evaluating large language models trained on code. *arXiv preprint arXiv:2107.03374*, 2021.
- Karl Cobbe, Vineet Kosaraju, Mohammad Bavarian, Mark Chen, Heewoo Jun, Lukasz Kaiser, Matthias Plappert, Jerry Tworek, Jacob Hilton, Reiichiro Nakano, et al. Training verifiers to solve math word problems. *arXiv preprint arXiv:2110.14168*, 2021.
- DeepSeek-AI. Deepseek-r1: Incentivizing reasoning capability in llms via reinforcement learning. *arXiv preprint arXiv:2501.12948*, 2025.
- Peng Ding, Jun Kuang, Dan Ma, Xuezhi Cao, Yunsen Xian, Jiajun Chen, and Shujian Huang. A wolf in sheep’s clothing: Generalized nested jailbreak prompts can fool large language models easily. In *Proceedings of the 2024 Conference of the North American Chapter of the Association for Computational Linguistics: Human Language Technologies (Volume 1: Long Papers)*, pages 2136–2153, 2024.
- Abhimanyu Dubey, Abhinav Jauhri, Abhinav Pandey, Abhishek Kadian, Ahmad Al-Dahle, Aiesha Letman, Akhil Mathur, Alan Schelten, Amy Yang, Angela Fan, et al. The llama 3 herd of models. *arXiv preprint arXiv:2407.21783*, 2024.
- Dario Garcia-Gasulla, Adrián Tormos, Anna Arias-Duart, Daniel Hinjos, Oscar Molina-Sedano, Ashwin Kumar Gurarajan, and Maria Eugenia Cardello. Efficient safety retrofitting against jailbreaking for llms. In *International Conference on Computer Safety, Reliability, and Security*, pages 537–565. Springer, 2025.
- Samuel Gehman, Suchin Gururangan, Maarten Sap, Yejin Choi, and Noah A Smith. Realtotoxicityprompts: Evaluating neural toxic degeneration in language models. In *Findings of the Association for Computational Linguistics: EMNLP 2020*, pages 3356–3369, 2020.
- Shaona Ghosh, Prasoon Varshney, Makesh Narsimhan Sreedhar, Aishwarya Padmakumar, Traian Rebedea, Jibin Rajan Varghese, and Christopher Parisien. Aegis2. 0: A diverse ai safety dataset and risks taxonomy for alignment of llm guardrails. In *Proceedings of the 2025 Conference of the Nations of the Americas Chapter of the Association for Computational Linguistics: Human Language Technologies (Volume 1: Long Papers)*, pages 5992–6026, 2025.
- Xuan Li, Zhanke Zhou, Jianing Zhu, Jiangchao Yao, Tongliang Liu, and Bo Han. Deepinception: Hypnotize large language model to be jailbreaker. In *Neurips Safe Generative AI Workshop 2024*, 2024.
- Stephanie Lin, Jacob Hilton, and Owain Evans. Truthfulqa: Measuring how models mimic human falsehoods. In *Proceedings of the 60th annual meeting of the association for computational linguistics (volume 1: long papers)*, pages 3214–3252, 2022.
- Xiaogeng Liu, Nan Xu, Muhao Chen, and Chaowei Xiao. Autodan: Generating stealthy jailbreak prompts on aligned large language models. In *The Twelfth International Conference on Learning Representations*, 2024.
- Chris Yuhao Liu, Liang Zeng, Yuzhen Xiao, Jujie He, Jiakai Liu, Chaojie Wang, Rui Yan, Wei Shen, Fuxiang Zhang, Jiacheng Xu, Yang Liu, and Yahui Zhou. Skywork-reward-v2: Scaling preference data curation via human-ai synergy. *arXiv preprint arXiv:2507.01352*, 2025.
- Huijie Lv, Xiao Wang, Yuansen Zhang, Caishuang Huang, Shihan Dou, Junjie Ye, Tao Gui, Qi Zhang, and Xuanjing Huang. Codechameleon: Personalized encryption framework for jailbreaking large language models. *arXiv preprint arXiv:2402.16717*, 2024.
- OpenAI. GPT-4 Technical Report, December 2023.

- Long Ouyang et al. Training language models to follow instructions with human feedback. In *Advances in Neural Information Processing Systems (NeurIPS)*, 2022.
- Hoang Phan, Victor Li, and Qi Lei. Think twice, generate once: Safeguarding by progressive self-reflection. In *Findings of the Association for Computational Linguistics: EMNLP 2025*, pages 9466–9483, 2025.
- Xiangyu Qi et al. Safety alignment should be made more than just a few tokens deep. In *ICLR*, 2025.
- Xiangyu Qi, Yi Zeng, Tinghao Xie, Pin-Yu Chen, Ruoxi Jia, Prateek Mittal, and Peter Henderson. Fine-tuning aligned language models compromises safety, even when users do not intend to! In *The Twelfth International Conference on Learning Representations*.
- Rafael Rafailov et al. Direct preference optimization: Your language model is secretly a reward model. In *NeurIPS*, 2023.
- Alexandre Sablayrolles, Matthijs Douze, Cordelia Schmid, and Hervé Jégou. Spreading vectors for similarity search. *arXiv preprint arXiv:1806.03198*, 2018.
- Xinyue Shen, Zeyuan Chen, Michael Backes, Yun Shen, and Yang Zhang. ”do anything now”: Characterizing and evaluating in-the-wild jailbreak prompts on large language models. In *Proceedings of the 2024 on ACM SIGSAC Conference on Computer and Communications Security*, pages 1671–1685, 2024.
- Rohan Taori, Ishaan Gulrajani, Tianyi Zhang, Yann Dubois, Xuechen Li, Carlos Guestrin, Percy Liang, and Tatsunori B Hashimoto. Stanford alpaca: An instruction-following llama model, 2023.
- Hugo Touvron, Louis Martin, Kevin Stone, Peter Albert, Amjad Almahairi, Yasmine Babaei, Nikolay Bashlykov, Soumya Batra, Prajjwal Bhargava, Shruti Bhosale, et al. Llama 2: Open foundation and fine-tuned chat models. *arXiv preprint arXiv:2307.09288*, 2023.
- Ivan Vykopal, Matúš Pikuliak, Ivan Srba, Robert Moro, Dominik Macko, and Maria Bielikova. Disinformation capabilities of large language models. In *Proceedings of the 62nd Annual Meeting of the Association for Computational Linguistics (Volume 1: Long Papers)*, pages 14830–14847, 2024.
- Alexander Wei et al. Jailbroken: How aligned language models can still be forced to deliver harmful content. In *ICLR*, 2024.
- Laura Weidinger, John Mellor, Maribeth Rauh, Conor Griffin, Jonathan Uesato, Po-Sen Huang, Myra Cheng, Mia Glaese, Borja Balle, Atoosa Kasirzadeh, et al. Ethical and social risks of harm from language models. *arXiv preprint arXiv:2112.04359*, 2021.
- An Yang, Baosong Yang, Beichen Zhang, Binyuan Hui, Bo Zheng, Bowen Yu, Chengyuan Li, Dayiheng Liu, Fei Huang, Haoran Wei, et al. Qwen2.5 technical report. *arXiv preprint arXiv:2412.15115*, 2024.
- Sibo Yi, Yule Liu, Zhen Sun, Tianshuo Cong, Xinlei He, Jiaying Song, Ke Xu, and Qi Li. Jailbreak attacks and defenses against large language models: A survey. *arXiv preprint arXiv:2407.04295*, 2024.
- Wenjun Zeng, Yuchi Liu, Ryan Mullins, Ludovic Peran, Joe Fernandez, Hamza Harkous, Karthik Narasimhan, Drew Proud, Piyush Kumar, Bhaktipriya Radharapu, Olivia Sturman, and Oscar Wahltinez. Shieldgemma: Generative ai content moderation based on gemma, 2024.
- Weikang Zhou, Xiao Wang, Limao Xiong, Han Xia, Yingshuang Gu, Mingxu Chai, Fukang Zhu, Caishuang Huang, Shihan Dou, Zhiheng Xi, Rui Zheng, Songyang Gao, Yicheng Zou, Hang Yan, Yifan Le, Ruohui Wang, Lijun Li, Jing Shao, Tao Gui, Qi Zhang, and Xuanjing Huang. Easyjailbreak: A unified framework for jailbreaking large language models, 2024.
- Andy Zou, Zifan Wang, Nicholas Carlini, Milad Nasr, J Zico Kolter, and Matt Fredrikson. Universal and transferable adversarial attacks on aligned language models. *arXiv preprint arXiv:2307.15043*, 2023.
- Andy Zou, Zifan Wang, J Zico Kolter, and Matt Fredrikson. Universal and transferable adversarial attacks on aligned language models. *arXiv preprint arXiv:2307.15043*, 2023.

Appendix

The appendix is organized as follows:

- **Appendix A** provides a detailed introduction to various adversarial attack methods and baselines.
- **Appendix B** describes the benchmark datasets utilized for safety and utility evaluation.
- **Appendix C** offers further elaboration on the definitions and mathematical relationship between latent content c and style s .
- **Appendix D** presents the rigorous mathematical proof of Theorem 1 regarding the identifiability of latent intent.
- **Appendix E** elucidates the causal assumptions (Independence and Connectivity) underlying the proposed TSC-GRPO framework.

A Introduction of Adversarial Attacks

- **GCG** Zou *et al.* [2023a]: A white-box suffix attack that performs gradient-guided coordinate updates over discrete tokens to search for an adversarial prompt suffix that maximizes harmful compliance under the target model.
- **AutoDAN** Liu *et al.* [2024]: An automated jailbreak method that optimizes stealthy “Do-Anything-Now”-style suffixes via iterative rewriting and selection to reliably elicit policy-violating responses.
- **ReNeLLM** Ding *et al.* [2024]: A prompt-based jailbreak that uses *generalized nested* instruction structures (e.g., multi-layer role-play / indirection) to hide malicious intent inside innocuous outer contexts, thereby bypassing safety filters and inducing harmful compliance.
- **CodeChameleon** Lv *et al.* [2024]: A jailbreak framework that obfuscates malicious instructions via *personalized encryption* and then guides the model to decrypt and execute the hidden intent in-context, making the attack adaptive and harder for surface-level safety checks to detect.
- **PAIR** Chao *et al.* [2025]: A black-box, query-efficient jailbreak that uses an attacker model to iteratively propose prompts and refine them using feedback from the target model’s responses within a limited query budget.
- **DeepInception** Li *et al.* [2024]: A prompt-based attack that nests the target instruction inside multi-layer role-play or “story-within-a-story” contexts to distract safety filters and elicit disallowed content.
- **Prefix Injection** Shen *et al.* [2024]: A prefix-based bypass that forces an initial compliant framing (e.g., “Sure, here is...”) or prefilled partial output so the model continues generation past the safety guardrails.
- **MSJ** Anil *et al.* [2024]: A many-shot jailbreaking paradigm that leverages long-context demonstrations of harmful question–answer pairs to condition the model into repeating the demonstrated unsafe behavior on a new target query.

B Benchmark Datasets

- **AdvBench** Chen *et al.* [2022]: A safety red-teaming benchmark consisting of 520 harmful instruction-style prompts, used to measure a model’s unsafe compliance under jailbreak attacks.
- **Alpaca** Taori *et al.* [2023]: A 52K-example synthetic instruction-following dataset of (instruction, optional input, response) pairs generated by a stronger teacher model, primarily used for supervised instruction tuning.
- **GSM8K** Cobbe *et al.* [2021]: A grade-school math word-problem QA benchmark with 8.5K multi-step arithmetic questions (7,473 train and 1,319 test), where the task is to produce the correct final numeric answer.
- **HumanEval** Chen [2021]: A code generation benchmark of 164 Python function-synthesis problems paired with unit tests, evaluated by functional correctness.
- **MBPP** Austin *et al.* [2021]: A program synthesis benchmark of 974 crowd-sourced Python tasks, each specified by a natural-language description and checked by automated test cases.
- **TruthfulQA** Lin *et al.* [2022]: A truthfulness QA benchmark of 817 questions spanning 38 categories, designed so that models trained to imitate web text tend to produce common misconceptions rather than truthful answers.

C Further Elaboration on c and s

In the context of text generation (LLMs), distinguishing between x and s is indeed far more challenging than in Computer Vision (CV). In CV, image pixels (x) and rotation angles (s) are clearly distinct entities. However, in NLP, the Token itself serves as both the object of observation and the carrier of style, which leads to the perception that they overlap.

To validate the mathematical theorem $x = f(c, s)$, we must draw a definitive boundary between the Latent Space and the Observation Space. We rigorously redefine these terms below to clarify their distinction.

C.1 Redefining the Relationship

We formalize the Large Language Model as a function f .

- **c (Latent Content Variable):**
 - **Definition:** The user’s original malicious intent.
 - **Example:** “Knowledge on how to make bombs.”
 - **Property:** Abstract and invisible.
- **s (Latent Style Variable):**
 - **Definition:** The current contextual environment (Prompt Template + Prefix).
 - **Examples:**
 - * s_1 : Question only.
 - * s_2 : Question + “Sure”.
 - * s_3 : Question + “Sure, here is”.
 - **Property:** The “cloak” or wrapper used to package the intent.
- **x (Observed Representation):**
 - **Definition:** The hidden state vector of a specific layer (typically the final transformer block output), e.g., with dimension $d = 4096$.
 - **Property:** The product of mixing c and s .

C.2 Why do x and s not overlap?

The key distinction is that s is the **Cause** (Ingredient), while x is the **Effect** (Result/Mixture).

The Cocktail Analogy:

- **c (Content):** Alcohol (The core ingredient to be extracted).
- **s (Style):** Juice, ice, lemon slices (Ingredients that alter taste and color).
- **x (Observation):** The mixed liquid in the glass.

Mapping this to the model: When the input changes to “Question + Sure”, the recipe’s style s is altered. The model computes and outputs a sequence of vectors, which is x .

1. x contains features of s (e.g., information expressing an “affirmative tone”).
2. x contains features of c (e.g., information regarding “bomb-making”).

The confusion arises because we observe Tokens (the manifestation of s) directly, making s appear equivalent to x . However, in this theoretical framework, we view Tokens merely as external interference factors. Our focus is on x as the “contaminated vector.”

Our goal, utilizing **Theorem 1**, is to find a transformation that filters out the “juice” (s) from the “cocktail” (x), retaining only the high-purity “alcohol” (c).

C.3 Mathematical Formulation

Let the observation at time t be defined as:

$$x_t = \text{LLM.Layer}(c, s_t) \quad (12)$$

where s_t denotes the combination of tokens (style) at time t , and x_t denotes the generated embedding vector.

Our objective is to train a mapping $g(\cdot)$ that is invariant to style changes. Even if s_1 (no prefix) transitions to s_2 (with “Sure” prefix), causing a drastic shift from x_1 to x_2 in the vector space, the mapping must satisfy:

$$g(x_1) \approx g(x_2) \approx c \quad (13)$$

This implies that regardless of how the context (s) varies, the extracted intent (c) must remain constant.

D Proof of Theorem 1

In this section, we provide a rigorous derivation of Theorem 1. We aim to show that minimizing the proposed objective function guarantees that the learned probe g^* recovers the latent content variable c up to an invertible transformation, while completely discarding the style variable s .

D.1 Problem Restatement

Let the observation be generated by a deterministic function $h = f(c, s)$, where $c \in \mathcal{C}$ is the latent intent (content) and $s \in \mathcal{S}$ is the nuisance style. We assume:

1. **Independence:** The joint distribution factorizes as $P(c, s) = P(c)P(s)$. This ensures that the support of the data covers the product space $\mathcal{C} \times \mathcal{S}$.
2. **Connectivity:** The augmentation graph $\mathcal{G}_{\mathcal{S}}$ is connected.

The training objective is:

$$\mathcal{L}(g) = \mathcal{L}_{align}(g) + \lambda \mathcal{L}_{unif}(g) \quad (14)$$

where $\mathcal{L}_{align} = \mathbb{E}_{c, s, s'} \|g(f(c, s)) - g(f(c, s'))\|^2$.

D.2 Step 1: Alignment Enforces Style Invariance

First, we analyze the behavior of the optimal probe g^* with respect to the Alignment Loss. Since $\mathcal{L}_{align} \geq 0$, the global minimum is achieved if and only if the term inside the expectation is zero almost everywhere.

Lemma 1 (Style Invariance). *If $\mathcal{L}_{align}(g^*) = 0$ and the Connectivity assumption holds, then $g^*(f(c, s))$ depends only on c . That is, there exists a function $\psi : \mathcal{C} \rightarrow \mathcal{Z}$ such that $g^*(f(c, s)) = \psi(c)$ for all $s \in \mathcal{S}$.*

Proof. Consider a fixed intent c . The alignment loss samples positive pairs by varying the style $s \rightarrow s'$ while keeping c fixed. The condition $\mathcal{L}_{align}(g^*) = 0$ implies:

$$g^*(f(c, s)) = g^*(f(c, s')) \quad \text{almost surely for } (s, s') \in \mathcal{E}_{\mathcal{G}} \quad (15)$$

where $\mathcal{E}_{\mathcal{G}}$ denotes the edges in the augmentation graph (pairs of styles constructed via our templates).

By the **Connectivity Assumption**, for any two arbitrary styles $s_a, s_b \in \mathcal{S}$, there exists a finite path of transitions $s_a \rightarrow s_1 \rightarrow s_2 \cdots \rightarrow s_b$. By transitivity of equality:

$$g^*(f(c, s_a)) = g^*(f(c, s_1)) = \cdots = g^*(f(c, s_b)) \quad (16)$$

Since this holds for any s_a, s_b , the value of $g^*(f(c, s))$ is constant with respect to s . Thus, g^* removes all information about s . We can simplify the probe as a function of c alone:

$$g^*(h) = \psi(c) \quad (17)$$

□

	Harmful Intent (c_{harm})	Safe Intent (c_{safe})
Style: Compliance (s_{sure})	Type II Harmful ($q_{harm} \oplus$ “Sure”)	Type II Safe ($q_{safe} \oplus$ “Sure”)
Style: Default (s_{raw})	Type I Harmful (q_{harm})	Type I Safe (q_{safe})

Table 4: The constructed intervention distribution enforcing independence.

D.3 Step 2: Uniformity Enforces Content Injectivity

From Step 1, we know the probe has collapsed the style dimension. However, a trivial solution $g^*(h) = \text{constant}$ (mapping all intents to a single point) also satisfies $\mathcal{L}_{align} = 0$. This is where the Uniformity Loss comes in.

Lemma 2 (Content Injectivity). *Minimizing \mathcal{L}_{unif} ensures that the function $\psi(c)$ is injective (invertible on its image).*

Proof. The KoLeo uniformity loss (and asymptotically, the maximization of differential entropy) minimizes the interaction energy between points. It is theoretically minimized when the distribution of outputs $z = g(h)$ is the Uniform distribution on the feature manifold (e.g., the hypersphere).

Recall that $z = \psi(c)$. The entropy of the output variable Z is related to the input C by:

$$H(Z) = H(\psi(C)) \quad (18)$$

From information theory, the entropy of a deterministic function of a random variable is maximized if and only if the function is **injective** (one-to-one).

- If ψ maps two distinct intents $c_1 \neq c_2$ to the same point z (feature collapse), the entropy $H(Z)$ strictly decreases because information about the distinction between c_1 and c_2 is lost.
- To minimize \mathcal{L}_{unif} (which is equivalent to maximizing entropy $H(Z)$), the optimal ψ^* must preserve all distinctions present in the input distribution $P(c)$.

Therefore, for distinct intents $c_i \neq c_j$, we must have $\psi^*(c_i) \neq \psi^*(c_j)$. This implies ψ^* is an invertible mapping. \square

D.4 Conclusion

Combining Lemma 1 and Lemma 2: 1. From Alignment: $g^*(f(c, s)) = \psi(c)$ (The probe ignores style). 2. From Uniformity: $\psi(c)$ is invertible (The probe distinguishes distinct intents).

Thus, the learned representation $z = g^*(h)$ is isomorphic to the true latent intent c . We can recover the intent via $c = \psi^{-1}(z)$. This completes the proof that minimizing the proposed objective guarantees the identifiability of the latent intent.

E Detailed Elucidation of Causal Assumptions

In Section 4, we invoked Theorem 1 to guarantee the identifiability of the latent intent variable c . This theorem relies on two structural assumptions regarding the data generation process: **Independence** and **Connectivity**. Here, we provide a detailed, intuitive explanation of why these assumptions are rigorously satisfied in our TSC-GRPO framework.

E.1 The Independence Assumption ($c \perp s$)

Intuition: Breaking Spurious Correlations. In the natural distribution of language (and in standard pre-training data), Content (c) and Style (s) are often highly correlated. For example, a polite prefix like “Sure, here is” ($s_{compliant}$) is statistically strongly correlated with helpful/safe content (c_{safe}). Conversely, refusals are correlated with harmful content. This statistical dependency is precisely why shallow alignment fails: the model learns to rely on the style s as a shortcut to predict the safety of c .

The Independence Assumption requires us to break this correlation, rendering the style variable s statistically uninformative about the content c . In other words, knowing the prefix is “Sure” should give the model zero information about whether the intent is harmful or safe.

Why it is satisfied by design? In our framework, this assumption is not merely an observation; it is a structural property enforced by construction via our data augmentation strategy. As detailed in Stage 1, we explicitly construct a balanced 2×2 contrastive matrix:

By feeding the probe samples from all quadrants of Table 4, we force the conditional probability $P(Intent|Style)$ to approach the marginal probability $P(Intent)$.

$$P(c_{harm}|s_{sure}) \approx P(c_{harm}|s_{raw}) \approx P(c_{harm}) \quad (19)$$

Because we artificially attach compliant prefixes to harmful queries (Malicious Compliance) and partial prefixes to safe queries, the probe cannot minimize the loss by relying on the prefix. It is mathematically compelled to look deeper for the invariant features of c , thus satisfying the independence assumption $c \perp s$.

E.2 The Connectivity Assumption (Augmentation Graph)

What is the Augmentation Graph? The Augmentation Graph \mathcal{G}_S is a conceptual graph where:

- **Nodes** represent different “views” or realizations of the same underlying intent (e.g., the raw query x_{raw} , the jailbroken query x_{sure} , the adversarial query x_{adv}).
- **Edges** represent the “positive pair” relationships. If our training objective pulls two views together (treating them as having the same intent), an edge exists between them.

The Connectivity Assumption states that this graph must be connected. This means there must be a path between any two styles s_i and s_j . If the graph were disconnected (e.g., two isolated islands), the probe could learn two separate, unrelated representations for the same intent, failing to unify them into a single concept c .

Why it is satisfied: The Star Topology. In the context of Contrastive Learning and our method, this assumption is trivially satisfied because our augmentation strategy follows a **Star Topology** (or Hub-and-Spoke model).

Consider a specific harmful intent c (e.g., “bomb making”). The “Center Node” (Hub) is the raw query q (Type I). All other augmented views are generated directly from this hub:

- Type II ($q \oplus$ “Sure”) is a perturbation of q . \rightarrow Edge (x_{raw}, x_{sure}) .
- Type III ($q \oplus \delta_{adv}$) is a perturbation of q . \rightarrow Edge (x_{raw}, x_{adv}) .
- Type IV ($q \oplus y_{1:k}$) is an extension of q . \rightarrow Edge $(x_{raw}, x_{partial})$.

Even if we do not explicitly pair Type II (Sure) and Type III (Adversarial) directly in a single triplet, they are linked via the Hub (x_{raw}).

$$x_{sure} \leftrightarrow x_{raw} \leftrightarrow x_{adv} \quad (20)$$

By transitivity, pulling x_{sure} close to x_{raw} and x_{raw} close to x_{adv} forces x_{sure} and x_{adv} to be close to each other. Therefore, as long as all augmentations share the original query q as their common source, the Augmentation Graph consists of a single connected component. There are no isolated subgraphs, guaranteeing that the probe learns a unified, globally consistent representation for the intent c .